

## Thermal Conductivity of Porous Media. I. Unconsolidated Sands

W. WOODSIDE AND J. H. MESSMER

*Gulf Research and Development Company, Pittsburgh, Pennsylvania*

(Received March 13, 1961)

The problem of determining the effective thermal conductivity of a two-phase system, given the conductivities and volume fractions of the components, is examined. Equations are described which have been proposed as solutions to this problem, including those of Maxwell, de Vries, and Kunii and Smith, the weighted geometric mean equation, and an equation based on a three-element resistor model found applicable to the analogous electrical conductivity problem. Experimental results are presented for five unconsolidated samples: three quartz sand packs, a glass bead pack, and a lead shot pack. The method of conductivity measurement using the transient line heat source (thermal conductivity probe) is described. Data are reported showing the variation of effective thermal conductivity with porosity, solid particle conductivity, saturating fluid conductivity, and the pressure of the saturating gas. From considerations based on the kinetic theory of gases, it is shown that the characteristic dimension of the pore space, with respect to heat conduction in the gas occupying this space, is smaller than the mean particle diameter by a factor of roughly 100. The thermal conductivity equations which best represent the observed data are those of de Vries, and Kunii and Smith, and a slightly modified version of the resistor model equation.

### INTRODUCTION

THE effective thermal conductivities of several unconsolidated sand packs and porous rocks have been measured under a variety of test conditions. The reason for the need for such data is the current interest in thermal methods of petroleum production from underground oil-bearing sands and rocks. Knowledge of the thermal properties of such porous materials is important in many other fields also. Calculations of heat dissipation from underground nuclear explosions and of the rate of heat loss from the earth due to the geothermal gradient depend directly upon the thermal conductivity values of the rocks involved. Determinations of the current-carrying capacity of buried cables and of the heat losses from underground steam and hot water pipes require values for the conductivities of soils. The design of packed columns, thermal insulating, and refractory materials depends upon the heat transfer characteristics of porous media.

Few reliable thermal data on petroleum reservoir-type rocks are presently available in the literature. The properties of interest are the thermal conductivity  $k$ , the thermal diffusivity  $\alpha$ , and specific heat  $c$ . Since these three quantities are interrelated, ( $\alpha = k/\rho c$ , where  $\rho$  is density) knowledge of any two determines the third. The heat capacity  $\rho c$  of a rock or sand of porosity  $\phi$  ( $\phi$  = fractional void volume =  $1$  - rock volume fraction), containing oil and water at saturations  $S_o$  and  $S_w$ , respectively, may be closely approximated by

$$\rho c = (1 - \phi)\rho_s c_s + \phi S_o \rho_o c_o + \phi S_w \rho_w c_w, \quad (1)$$

where  $c_s$ ,  $c_o$ , and  $c_w$  and  $\rho_s$ ,  $\rho_o$ , and  $\rho_w$  are the specific heats and densities of the solid, oil, and water, respectively, all of which are known or easily measured. Thus if the effective thermal conductivity  $k$  can be measured, the thermal diffusivity may be calculated.

In connection with thermal oil recovery processes the variation of effective thermal conductivity with the following parameters is required: (a) porosity,

(b) saturating fluid, (c) pressure of the saturating fluid, (d) over-burden pressure, and (e) temperature.

In addition to providing reliable thermal conductivity data, it is desirable to find a correlation, empirical or otherwise, between conductivity and other more easily measured parameters such as porosity, formation factor (formation factor = resistivity of a rock 100% saturated with fluid of resistivity  $R_w \div R_o$ ), etc. Many of the equations proposed for the thermal conductivity of a heterogeneous system have therefore been examined in terms of the data presented herein.

This present paper describes the theoretical background, the method of conductivity measurement, and the results for unconsolidated media. A second paper will describe the results obtained for consolidated porous rocks.

### THEORY

Consider any two-phase porous material, i.e., one consisting of a single solid component (subscript  $s$ ) and a single saturating fluid in the pore space (subscript  $f$ ). The effective thermal conductivity  $k$  of such a material depends on the following parameters: (a) the thermal conductivities of the two phases,  $k_s$  and  $k_f$ , (b) the volume concentrations of the two phases,  $(1 - \phi)$  and  $\phi$ , where  $\phi$  is the fractional porosity, and (c) the distribution of the two phases in the material. The effective conductivity will also depend upon the particle or pore size, at high temperatures when radiative heat transfer in a gaseous fluid is not negligible, or when the pore sizes are large enough that convection heat transfer may occur. Both of these mechanisms are neglected in this work, since the measurements to date have been performed at room temperature on samples none of which contained pores large enough to permit convection.

It is convenient to introduce the following dimensionless conductivity ratios:

$$x = k_s/k_f \quad y = k/k_f. \quad (2)$$

The above statement is equivalent to

$$y = F(x, \phi, \text{phase distribution}). \quad (3)$$

The problem of determining the functional relationship denoted by  $F$ , for a given phase distribution, is the same whether the  $k$  symbols represent thermal conductivities, electrical conductivities, diffusion coefficients, dielectric constants, or permeabilities.

For all cases considered here,  $k_f < k_s$ , and therefore  $k_f < k < k_s$ , or  $1 < y < x$ . However, closer and much more useful limits may be placed on  $k$ , by considering two very simple phase distributions. These are the series and parallel distributions, which correspond to the minimum and maximum values of  $y$ , respectively, for given values of  $x$  and  $\phi$ .

The series distribution, in which the two phases are thermally in series with respect to the direction of heat flow, results in the following:

$$k_{\min} = k_s k_f / [\phi k_s + (1 - \phi) k_f] \quad (4)$$

or

$$y_{\min} = x / [\phi(x - 1) + 1].$$

The parallel distribution, in which the two phases are thermally in parallel with respect to the direction of heat flow, results in the following:

$$k_{\max} = \phi k_f + (1 - \phi) k_s \quad (5)$$

or

$$y_{\max} = \phi + (1 - \phi)x.$$

It should be noted that for both distributions

$$\left( \frac{dk}{dk_s} \right)_{k_s=k_f} = 1 - \phi \quad (6)$$

or

$$\left( \frac{dy}{dx} \right)_{x=1} = 1 - \phi.$$

The fact that the equations for maximum and minimum conductivity both satisfy the relationship (6) means that the conductivity equation for any phase distribution must also satisfy it.

The parallel distribution (maximum  $k$ ) corresponds to a weighted arithmetic mean of the conductivities of the two phases; the series distribution (minimum  $k$ ) corresponds to the weighted harmonic mean of the solid and fluid conductivities. It is interesting to consider how the intermediate weighted geometric mean represents the conductivity of a natural porous medium. The weighted geometric mean corresponds to

$$k = k_f^\phi k_s^{1-\phi} \quad (7)$$

or

$$y = x^{1-\phi}.$$

It is easily shown that this simple equation satisfies the required condition (6) as it must if it is to be a valid conductivity equation.

The properties of the three equations dealt with so far are summarized in the following table.

Minimum $k$	Intermediate $k$	Maximum $k$
$\phi/k_f + (1 - \phi)/k_s$	$k = k_f^\phi k_s^{1-\phi}$	$k = \phi k_f + (1 - \phi) k_s$
Series distribution Harmonic mean	Random distribution Geometric mean	Parallel distribution Arithmetic mean

The proposed geometric mean equation (7) corresponds to a weighted arithmetic mean of the logarithms of the individual conductivities.

$$\log k = \phi \log k_f + (1 - \phi) \log k_s. \quad (8)$$

In other words, this equation predicts a linear relationship, on a log-log plot, between the effective conductivity of a porous medium and the conductivity of the fluid saturant.

Asaad<sup>1</sup> has proposed an empirical relationship which is very similar to the geometric mean equation.

Asaad's equation is

$$k/k_s = (k_f/k_s)^m, \quad (9)$$

where  $m = c\phi$  and  $c \cong 1$ . If  $c = 1$ , this equation is identical to the geometric mean equation. Somerton<sup>2</sup> has attempted to correlate his conductivity data by means of Asaad's equation. Legg and Given<sup>3</sup> have also used an empirical relationship similar to the geometric mean equation for the analogous dielectric constant problem. The geometric mean is also a first term approximation to a solution of Brown's<sup>4</sup> for solid mixture permittivities. Recently Langton and Matthews<sup>5</sup> have applied the geometric mean equation in its logarithmic form, Eq. (8), to the calculation of the permittivity of mixtures of zinc oxide and rubber, the calculated values agreeing quite well with those measured. These authors attribute the equation to Lichteneker<sup>6</sup> who obtained it empirically in 1926.

Maxwell's<sup>7</sup> equation for the electrical conductivity of a random distribution of solid spheres ( $k_s$ ) in a continuous medium ( $k_f$ ) may be shown to be equivalent to

$$k = k_f \left[ \frac{2\phi k_f + (3 - 2\phi) k_s}{(3 - \phi) k_f + \phi k_s} \right]. \quad (10)$$

This equation is strictly applicable only when  $\phi$  is large, since it was derived on the assumption that the solid spheres are far enough apart that they do not mutually interact. Eucken<sup>8</sup> generalized Maxwell's equa-

<sup>1</sup> Y. Asaad, Ph.D. thesis, University of California, June, 1955.

<sup>2</sup> W. H. Somerton, *J. Petrol. Technol.* **10**, 61 (1958).

<sup>3</sup> V. E. Legg, and F. J. Given, *Bell System Tech. J.* **19**, 385 (1940).

<sup>4</sup> W. F. Brown, Jr., *J. Chem. Phys.* **23**, 1514 (1955).

<sup>5</sup> N. H. Langton and D. Matthews, *Brit. J. App. Phys.* **10**, 306 (1959).

<sup>6</sup> K. Lichteneker, *Z. Physik.* **27**, 115 (1926).

<sup>7</sup> J. C. Maxwell, *A Treatise on Electricity and Magnetism* (Clarendon Press, Oxford, England, 1904), 3rd ed., Vol. 1, p. 440.

<sup>8</sup> A. Eucken, *Forsch. Gebiete Ingenieurw.* **B3**, VDI-Forschungsheft, 353 (1932).

tion to the case of  $n$  dispersed phases and one continuous phase and applied the resulting equation to the thermal conductivity problem.

de Vries<sup>9</sup> has applied Eucken's and Burger's extensions (to ellipsoidal particles) of Maxwell's equation to the calculation of unconsolidated soil thermal conductivities, the calculated values agreeing quite well with experimental data.<sup>9-11</sup> The equation for a two-phase medium with continuous fluid phase and dispersed solids is

$$k = \frac{\phi k_f + (1-\phi)F_1 k_s}{\phi + (1-\phi)F_1},$$

where

$$F_1 = \frac{1}{3} \sum_{i=1}^3 [1 + (k_s/k_f - 1)g_i]^{-1} \quad (11)$$

and

$$\sum_{i=1}^3 g_i = 1.$$

The factor  $F_1$  represents the ratio of the average temperature gradients in the continuous and dispersed phases. The factors  $g_i$  are particle shape factors. When  $g_1 = g_2 = g_3$  (spherical particles) the equation reduces to Maxwell's original equation. de Vries chose  $g_1 = g_2 = \frac{1}{8}$ , and  $g_3 = \frac{3}{4}$ . This corresponds to particles having the shape of ellipsoids of revolution with a major axis six times the minor axis.

Both Maxwell's and de Vries' equations satisfy the required condition (6), and furthermore all the preceding conductivity equations, except Asaad's, satisfy the requirements: (a) as  $\phi \rightarrow 0$ ,  $k \rightarrow k_s$  and (b) as  $\phi \rightarrow 1$ ,  $k \rightarrow k_f$ . Asaad's equation satisfies these requirements only if  $c=1$ .

Kunii and Smith<sup>12</sup> have extended the work of Yagi and Kunii<sup>13</sup> on packed beds, and propose the following equation for the conductivity of an unconsolidated granular material, neglecting radiation and heat conduction through the grain contacts (which will be shown later to be a close approximation).

$$k/k_f = \phi + [(1-\phi)/(\epsilon + \frac{2}{3}k_f/k_s)], \quad (12)$$

$$\epsilon = \epsilon_2 + (\phi - 0.259)(\epsilon_1 - \epsilon_2)/0.217.$$

where

The values of the parameters  $\epsilon_1$  and  $\epsilon_2$  are plotted as functions of  $k_s/k_f$  by Kunii and Smith.  $\epsilon_1$  corresponds to a cubic packing of uniform spheres ( $\phi=0.476$ ) and  $\epsilon_2$  corresponds to a tetrahedral packing of uniform spheres ( $\phi=0.259$ ). For intermediate porosities they calculate  $\epsilon$  by linear interpolation between  $\epsilon_1$  and  $\epsilon_2$ . For porosities less than 0.259 they recommend taking  $\epsilon$  to be equal to  $\epsilon_2$ , and for  $\phi > 0.476$ ,  $\epsilon = \epsilon_1$ . Wyllie and

<sup>9</sup> D. A. de Vries, Mededelingen van de Landbouwhogeschool te Wageningen (1952).

<sup>10</sup> W. Woodside and J. B. Cliffe, Soil Science 87, 75 (1959).

<sup>11</sup> W. Woodside and C. M. A. de Bruyn, Soil Science 87, 166 (1959).

<sup>12</sup> D. Kunii and J. M. Smith, A. I. Ch. E. Journal 6, 71 (1960).

<sup>13</sup> S. Yagi and D. Kunii, A. I. Ch. E. Journal 3, 373 (1957).

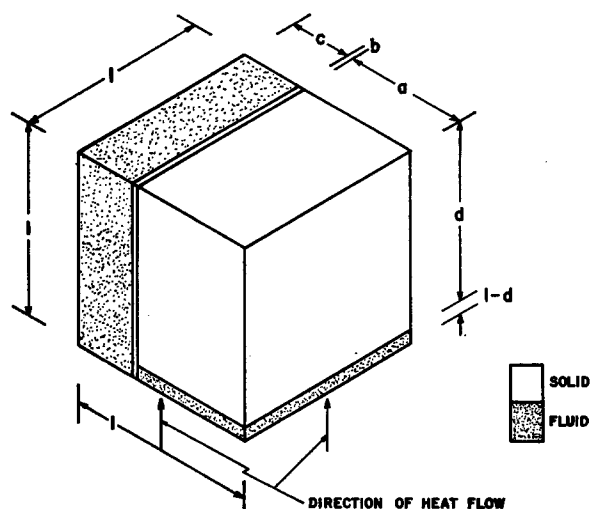


FIG. 1. Three-element resistor model of porous medium (Wyllie & Southwick).

Southwick<sup>14</sup> suggested that the electrical conductivity of an aggregate of conductive particles saturated with a conducting electrolyte was compatible with an equivalent resistor model comprising three elements in parallel, as shown in Fig. 1. The three components of electrical conductivity suggested were (1) an element  $k_1$ , comprising particles and electrolyte in series with each other, (2) an element  $k_2$ , consisting of particles in sufficiently close contact with each other to form continuously conducting paths, and (3) an element  $k_3$ , consisting of the electrolyte filling the interstices between the particles. It was assumed that  $k_1$ ,  $k_2$ , and  $k_3$  were in parallel. The model is thus a combination of the series and parallel distributions considered earlier. It follows from Fig. 1 that  $k$ , the effective conductivity of the aggregate, is given by

$$k = \frac{ak_s k_f}{k_s(1-d) + dk_f} + bk_s + ck_f, \quad (13)$$

where  $a+b+c=1$ . If the solids are nonconductive ( $k_s=0$ ), only element 3 contributes to the over-all conductivity, i.e.,  $k=ck_f$ . Therefore

$$c = 1/F, \quad (14)$$

where  $F$  is the electrical resistivity formation factor, defined as the ratio of the resistivity of a porous material fully saturated with an electrolyte to the resistivity of the electrolyte. This factor is used widely in the oil industry to characterize the pore structure of sedimentary rocks and sands. The relationship between  $F$  and the porosity  $\phi$  is well established for both consolidated and unconsolidated media.<sup>15</sup>

<sup>14</sup> M. R. J. Wyllie and P. F. Southwick, J. Petrol. Technol. 6, 44 (1954).

<sup>15</sup> M. R. J. Wyllie and A. R. Gregory, Petrol. Trans. Am. Inst. Min., Met., Petrol. Engrs. 198, TP 3541 (1953).

Sauer *et al.*<sup>16</sup> found the above resistor model to be consistent with their electrical conductivity data for aggregates of ion exchange resin particles saturated with several electrolytes.

The model may also be applied to the analogous thermal conductivity problem with which we are concerned here. From Fig. 1 it is apparent that

$$ad + b = 1 - \phi. \quad (15)$$

This relationship also follows directly from Eq. (13) by application of the required condition (6). Similarly, the relation  $a + b + c = 1$  also follows from Eq. (13) by applying the condition that when  $k_s = k_f$ ,  $k$  must also equal  $k_f$ . A fourth relationship is required in order to determine the four constants  $a$ ,  $b$ ,  $c$ , and  $d$  for a given material. From Eq. (13) it is evident that when  $k_f = 0$ ,  $k = bk_s$ ; this is the second element of the model, representing the "straight-through" solid conduction. The condition,  $k_f = 0$  may be closely approximated by evacuating the medium. Thus the value of the parameter  $b$  should be given by

$$b = k_{vac}/k_s. \quad (16)$$

It is hoped that an empirical relationship may be established between  $b$  and  $\phi$ , corresponding to the already established formation factor-porosity relationship. In fact, the similarity between the two parameters  $b$  and  $c$  is rather striking.

$$b = k(k_f = 0)/k_s; \quad c = k(k_s = 0)/k_f. \quad (17)$$

For consolidated rocks,  $1/F = c \cong 4/3\phi^2$ . It might perhaps be expected then, by analogy, that  $b = b'(1 - \phi)^2$ , where  $b'$  is independent of porosity. For unconsolidated media,  $1/F = c \cong \phi^{0.3}$ <sup>17</sup> or  $1/F = c \cong \phi/(1.3219 - 0.3219\phi)^2$ .<sup>18</sup>

Kimura<sup>19</sup> has applied the resistor model equation to the calculation of thermal conductivities of some unconsolidated packed beds. He assumed  $b = 0$  and  $c = \phi^{1.3}$  but did not use the relationship (15); instead he calculated the value  $d$  must have to make the model consistent with experimental data, correlating  $d/\phi^{1.5}$  with  $k_f/k_s$ .

Many other equations have been proposed for the thermal conductivity of a multiphase system, e.g., those of Gemant,<sup>20</sup> Russell,<sup>21</sup> Topper,<sup>22</sup> and Kersten.<sup>23</sup> However, these equations are not strictly applicable to the specific systems of interest here.

One difficulty in using the above equations for the calculation of thermal conductivities of such systems as rocks and sands is the assignment of the proper

value to  $k_s$ , the conductivity of the solid component. Whereas the conductivities  $k_f$  of all the fluid saturants of interest are well known, there is some doubt as to the conductivity attributable to the solid component of rocks, especially in the case of well-cemented rocks, where the cementing material, in the case of quartzitic sandstones, may have a conductivity quite different from that of the quartz particles. Furthermore, quartz is highly anisotropic, having a conductivity in the direction of the crystal axis twice that in the direction perpendicular to the crystal axis.<sup>24</sup> In a random distribution of crystal axis orientations, it is assumed that the average quartz conductivity is the arithmetic mean of these two values. For all quartzitic materials considered in this work, a value for  $k_s$  of  $20 \times 10^{-3}$  cal/cm sec°C at room temperature (i.e., 20 mcal/cm sec°C) has been assumed.

## EXPERIMENTAL

Many experimental investigations have already been made of the thermal conductivities of rocks and sands. Niven,<sup>25</sup> Birch and Clark,<sup>26</sup> Zierfuss and van der Vliet,<sup>27</sup> Benfield,<sup>28</sup> Beck,<sup>29,30</sup> Asaad,<sup>1</sup> and Somerton<sup>2</sup> have presented data of interest from both the geophysical and oil production standpoints. Kannuluik and Martin,<sup>31</sup> Schuman and Voss,<sup>32</sup> Kling,<sup>33</sup> Waddams,<sup>34</sup> Kimura,<sup>19</sup> and van Rooyen and Winterkorn<sup>35</sup> have presented data for unconsolidated packed beds. In many cases, the results were not interpreted in terms of the properties and concentrations of the constituent materials; in others, the range of porosity studied was narrow. Niven, Birch and Clark, and Somerton have investigated the effect of temperature; however, there has been no detailed study of the effects of gas pressure or overburden pressure.

The conventional methods of thermal conductivity measurement are steady-state methods. These involve the simultaneous measurement of the steady-state heat flux and temperature gradient through test samples in the form of slabs, cylinders, or spheres, for which solutions to the differential equation of heat conduction are readily available. Since no perfect thermal insulation exists, complicated guarding systems are required to minimize edge or end effects. A further drawback

<sup>24</sup> E. H. Ratcliffe, Brit. J. Appl. Phys. **10**, 22 (1959).

<sup>25</sup> C. D. Niven, Can. J. Research **A18**, 132 (1940).

<sup>26</sup> F. Birch and H. Clark, Am. J. Sci. **238**, 529 and 613 (1940).

<sup>27</sup> H. Zierfuss and G. van der Vliet, Bull. Am. Assoc. Petrol. Geologists **40**, 2475 (1956).

<sup>28</sup> A. E. Benfield, Proc. Roy. Soc. (London) **A-173**, 428 (1939).

<sup>29</sup> A. E. Beck, J. C. Jaeger, and G. Newstead, Australian J. Phys. **9**, 296 (1956).

<sup>30</sup> A. E. Beck and J. M. Beck, Trans. Am. Geophys. Union **39**, 111 (1958).

<sup>31</sup> W. G. Kannuluik and L. H. Martin, Proc. Roy. Soc. (London) **A141**, 144 (1933).

<sup>32</sup> T. E. W. Schumann and V. Voss, Fuel **13**, 249 (1934).

<sup>33</sup> G. Kling, Forsch. Gebiete Ingenieurw. **9**, 28 (1938).

<sup>34</sup> A. L. Waddams, J. Soc. Chem. Ind. (London) **63**, 337 (1944).

<sup>35</sup> M. van Rooyen and H. F. Winterkorn, Proc. Highway Research Board **38**, 376 (1959).

<sup>16</sup> M. C. Sauer, P. F. Southwick, K. S. Spiegler, and M. R. J. Wyllie, Ind. Eng. Chem. **47**, 2187 (1955).

<sup>17</sup> G. E. Archie, Petrol. Trans. Am. Inst. Min., Met., Petrol. Engrs. **146**, 54 (1942).

<sup>18</sup> A. Slawinski, J. chim. phys. **23**, 710 (1926).

<sup>19</sup> M. Kimura, Kagaku Kikai **21**, 472 (1957).

<sup>20</sup> A. Gemant, J. Appl. Phys. **21**, 750 (1950).

<sup>21</sup> H. W. Russell, J. Am. Ceram. Soc. **18**, 1 (1935).

<sup>22</sup> L. Topper, Ind. Eng. Chem. **49**, 1936 (1957).

<sup>23</sup> M. C. Kersten, Univ. of Minnesota, Eng. Expt. Sta. Bull. **28** (1949).

common to all steady-state methods is the relatively long time required to attain thermal equilibrium. In the case of porous media, containing partial liquid saturations, many difficulties are encountered. The application of the temperature gradient for a long period of time results in a nonuniform liquid saturation distribution due to the effects of thermal osmosis.<sup>10,11,36</sup> The conductivity so measured may depend upon the sample size and the magnitude of the temperature difference applied.

In contrast with steady-state methods, transient methods are fast and therefore less likely to produce nonuniform saturation distributions in the case of partially saturated rocks. The method used in the present work is the transient line heat source ("probe" or "needle") method originated by Stalhane and Pyk<sup>37</sup> and van der Held and van Drunen<sup>38</sup> for the measurement of thermal conductivity of liquids. The method uses a line heat source, i.e., a straight wire through which is passed a constant electric current, and a temperature-sensitive device, e.g., a thermocouple, thermistor, or resistance thermometer. These two elements are embedded alongside each other in the sample under test. When the assembly is at a uniform and constant temperature, constant power is supplied to the heater element and the rise in temperature is recorded during a short heating interval. The rate of rise of temperature is determined by the ability of the test sample to conduct the heat generated away from the line source. The thermal conductivity of the sample may be calculated from the temperature-time record and the power input. The theory on which the method is based is developed by Carslaw and Jaeger.<sup>39</sup>

The temperature rise  $\theta$  at a point in an infinite mass of material heated by a perfect line source is

$$\theta(r,t) = (Q/2\pi k) I[r/2(\alpha t)^{1/2}], \quad (18)$$

where  $Q$  = power input per unit length of source, cal/cm sec,  $k$  = thermal conductivity of material, cal/cm sec°C,  $\alpha$  = thermal diffusivity of material, cm<sup>2</sup>/sec,  $r$  = radial distance of point from line source, cm,  $t$  = time from start of heating, sec, and

$$I(x) = C - \ln x + \frac{x^2}{2} - \frac{x^4}{8} + \dots,$$

where  $C$  is Euler's constant (0.5772).

If  $x = [r/2(\alpha t)^{1/2}]$  is small, i.e., large  $t$  and small  $r$ , the terms of order  $x^2$  and above may be neglected and

$$\theta = (Q/2\pi k) \left[ C - \ln \frac{r}{2(\alpha t)^{1/2}} \right]. \quad (19)$$

Between times  $t_1$  and  $t_2$ , the temperature rise  $\Delta\theta$  is therefore given by

$$\Delta\theta = \theta_2 - \theta_1 = (Q/4\pi k) \ln(t_2/t_1) \quad (20)$$

or

$$k = (Q/4\pi\Delta\theta) \ln(t_2/t_1).$$

The thermal conductivity may also be evaluated by measuring the slope  $(Q/4\pi k)$  of the straight line obtained by plotting temperature rise  $\theta$  versus  $\ln t$ .

There are several sources of error in the method: (a) The first is the error due to dropping the higher terms in the  $I(x)$  series. This error is minimized by having the thermocouple close to the heater and by discounting the early part of the temperature-time record. (b) Secondly, the theory applies to a perfect line heat source, i.e., one with an infinitely large length to diameter ratio. Blackwell<sup>40</sup> has shown theoretically that probes with a length to diameter ratio of 30 or more will have negligible errors in this respect. (c) The theory also applies to a sample infinite in extent. However, if the testing interval is limited to the time before the heating effect is "felt" at the sample surface, then samples of practical dimensions behave as though they are infinite in size. (d) An error also arises due to the contact resistance between the probe and the surrounding sample. (e) Finally, there is an error due to variation in the resistance of the heater wire with temperature (nonconstant power input). This error can also be made negligible by using as the heater a wire with a low temperature coefficient of resistance.

For reasons of strength and ease of handling, the heater wire and thermocouple are usually encased in a protective metal sheath, and in this form the instrument has been called a thermal conductivity probe.<sup>41</sup> Probes have become quite popular in recent years for the measurement of thermal conductivity of thermal insulating materials and unconsolidated soils. The probe method does not appear to have been applied to rock conductivity measurements.

There are two conflicting requirements governing the size of a probe. To approximate an ideal line heat source the probe should have a large length to diameter ratio. On the other hand, thin probes produce large temperature gradients in the sample close to the probe, and may suffer from the same disadvantages as the steady-state methods, although to a lesser degree, with respect to thermal osmosis effects.<sup>42</sup>

## DESCRIPTION OF PROBE

A schematic diagram of the probe design is shown in Fig. 2. The probe has a length of 6 in. and an outside diameter of 0.065 in. (16 gauge tubing), giving a length

<sup>36</sup> J. R. Philip and D. A. de Vries, *Trans. Am. Geophys. Union* **38**, 222 (1957).

<sup>37</sup> B. Stalhane and S. Pyk, *Tek. Tidskl.* **61**, 29, 389 (1931).

<sup>38</sup> E. F. M. van der Held and F. G. van Drunen, *Physica* **15**, 865 (1949).

<sup>39</sup> H. S. Carslaw and J. C. Jaeger, *Conduction of Heat in Solids* (Clarendon Press, Oxford, England, 1959), 2nd ed.

<sup>40</sup> J. H. Blackwell, *Can. J. Phys.* **34**, 412 (1956).

<sup>41</sup> F. C. Hooper and F. R. Lepper, *Am. Soc. Heating Ventilating Engrs. Trans.* **56**, 309 (1950).

<sup>42</sup> W. Woodside, *Heating, Piping, Air Conditioning* **30**, 163 (1958).

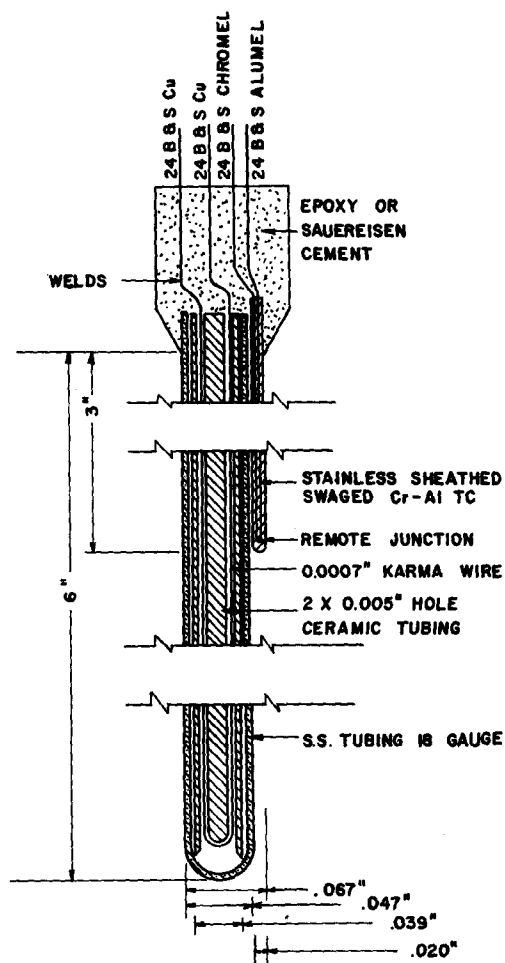


FIG. 2. Schematic diagram of thermal conductivity probe.

to diameter ratio of close to 100. The metal sheath is stainless steel hypodermic needle tubing (o.d. 0.065 in., i.d. 0.047 in.). The thermocouple is 0.003-in. copper-Constantan or Chromel-Alumel, with the thermojunction located at the mid-length of the probe. The heater wire is 0.0007-in. Karma (Driver-Harris Company) resistance wire, with a temperature coefficient of resistance of  $0.00002/^{\circ}\text{C}$ , and a resistance of 1633 ohms per foot of length. In the earlier probes the heater wire and thermocouple were enclosed in fine glass capillary tubes which were in turn enclosed in the metal tubing. The more recently built probes have had the four wires enclosed in a four-hole ceramic insulating tube with an o.d. of 0.045 in., which is inserted into the metal tubing. In all cases, one end of the metal tubing is sealed off and the four wires brought out to the other end and welded to heavier lead wires, the joint being strengthened by epoxy resin or Sauereisen cement. Some of the more recent tests have been conducted with a thermocouple attached to the outside surface of the metal tubing at its mid-length, resulting in a smoother temperature-time record (this design is shown in Fig. 2).

### PROBE CIRCUITRY

The circuit used in association with the probe is shown in Fig. 3. The power source is a regulated dc power supply with output voltage continuously variable from 0 to 400 vdc and maximum current load of 200 ma. The heating current  $i$  is obtained by measuring the potential drop across a 1-ohm standard resistance in series with the probe heater (resistance approximately 1600 ohms) with a portable potentiometer of 160 mv range, readable to  $1\mu\text{v}$ . The reference junction of the probe thermocouple is sometimes attached to the outer surface of the sample and other times is located in a Dewar flask containing room temperature water. The emf corresponding to the probe temperature rise is amplified and then recorded on a single-point Speedomax recorder with a range of  $-0.1$  to  $+1.0$  mv, and a chart speed of approximately 3 in./min. The preamplifier has a maximum gain of 200, is zero-center, and has ranges of 50, 100, 200, 500, 1000, and 2000  $\mu\text{v}$ .

The initial temperature rise (during the first 30 sec of heating for the probe design used here) cannot be used for calculating conductivity because of error (a) discussed above. Unfortunately a large fraction of the total temperature rise occurs during this time. It is therefore convenient to have a bias circuit built into the probe thermocouple circuit, permitting this first unusable part of the temperature time record to be biased out, and the remaining useful part of the record to be further amplified and spread across the full width of the recorder chart, thus increasing the accuracy. This is permissible, since the calculation of  $k$  involves only the difference in temperature rises at two times, and not the absolute value of the rises [Eq. (20)].

### EXPERIMENTAL PROCEDURE

In the case of unconsolidated samples, the material was packed into a cylindrical container of inside diameter 5 in. and inside height of 7 in., and the probe inserted in the center.

When the sample-probe system attained thermal equilibrium, as registered by a constant thermocouple reading, the current to the probe heater was switched on and the temperature rise recorded. The initial rise was biased out and the amplifier gain increased after

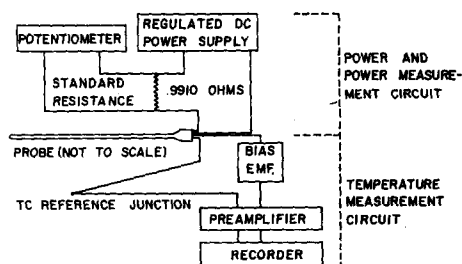


FIG. 3. Schematic circuit for probe thermal conductivity measurements.

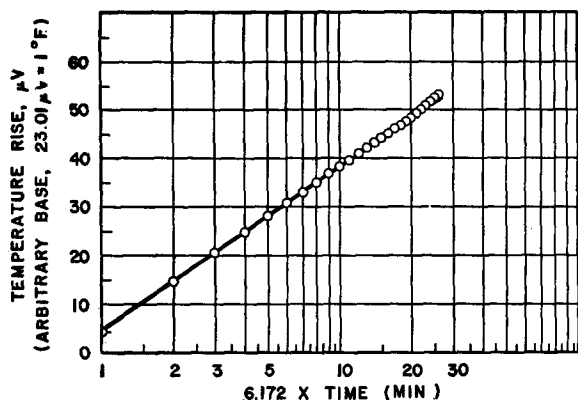


FIG. 4. Typical plot of probe temperature rise against logarithm of time from start of heating.

30 sec of heating as described above. Each measurement lasted approximately 3 min. During a test the current seldom changed by more than 0.1 percent. The final temperature rise at the probe was usually of the order of 5°C. All measurements were conducted near room temperature.

A sample plot of temperature rise versus the logarithm of the time from start of heating is shown in Fig. 4. The linearity of this plot is probably the best guarantee that the errors mentioned earlier are negligible, and that the probe in the vicinity of its mid-length is indeed behaving like a perfect line heat source.

The specific formula for the calculation of thermal conductivity from the probe data depends upon the calibration of the thermocouple used and also the resistance per unit length of the heater wire. For the probes used in this work, the formula is

$$k = \frac{0.1947 i^2 \log(t_2/t_1)}{V_2 - V_1} \text{ mcal/cm sec}^\circ\text{C}, \quad (21)$$

where  $i$  = heating current (ma) and  $V_2$ ,  $V_1$  = temperature rises ( $\mu\text{V}$ ) at times  $t_2$  and  $t_1$ .

The sample, probe, and sample container were placed inside a steel vessel with vacuum, gauge, and gas inlet connections. The probe leads were brought out through a Conax fitting in the top plate of the vessel.

In performing conductivity measurements as a function of air pressure, the sample was first evacuated and then air was allowed to leak in through a drying column to the desired pressure. To change from one gaseous saturant to another, the sample was evacuated, then filled with the desired gas to a pressure of one atmosphere, this process being repeated several times to ensure the purity of the gas in the sample.

Liquid saturations were achieved by vacuum saturation, the porosity of the sample being determined at the same time by weighing the sample before and after saturation.

## ACCURACY AND REPRODUCIBILITY

To determine the reproducibility of the method, the conductivity of a foamed plastic insulation sample was measured several times, each time modifying some component of the equipment. The conductivity measured varied by only 2.5 percent, with two different probes, two different power sources, three different biasing circuits, with and without mercury surrounding the projecting probe head. Reproducibility of better than 2.5 percent was obtained in the sand and rock conductivity measurements.

Measurements were also made on several "standard" insulation samples, the results showing excellent agreement with values reported in the literature.

## DESCRIPTION OF UNCONSOLIDATED SAMPLES

Measurements were made on three quartz sand packs, a glass bead pack, and a lead shot pack. The 59% porosity sand was a loose pack of 140/200 mesh (0.104–0.074 mm) Wassau quartz sand. The 36% porosity sand was a pack of 20/30 mesh (0.84–0.59 mm) Ottawa sand. The 19% porosity sand was a mixture of the 20/30 and 140/200 mesh sands packed in the following way. The 20/30 sand was packed alone into a Lucite container to a porosity of 31.5%; 140/200 mesh sand was then vibrated through an intermediate size mesh into the coarse sand pack until no more would enter.  $k_s$  for all three sand packs was assumed to be 20 mcal/cm sec°C.

The glass bead pack and the lead shot pack both had a porosity of 38%. The glass beads (Microbeads 405) are approximately 40/50 mesh (0.42–0.297 mm) and, according to the manufacturer, have a solid thermal conductivity of 2.5 mcal/cm sec°C, ( $k$ , mcal/cm sec°C  $\times 0.242 = k$ , Btu/hr ft°F). The mean particle diameter of the lead shot was 1.23 mm; the thermal conductivity of lead at 30°C is 82.0 mcal/cm sec°C.

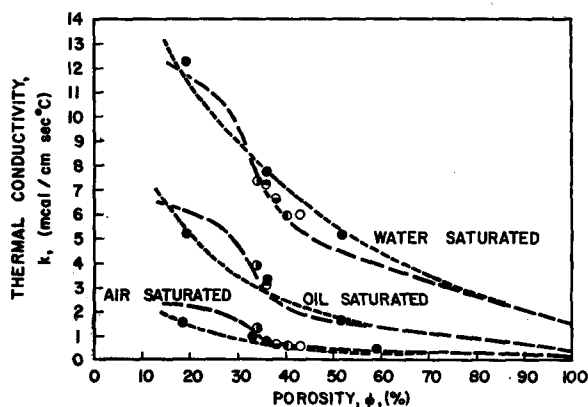


FIG. 5. Thermal conductivity of quartz sand packs as a function of porosity and saturating fluid. ● Probe data—Ottawa & Wassau sands; ○ DeVries—Wageningen sand<sup>9</sup>; ● Somerton—quartz sand<sup>2</sup>; ● Van Rooyen—white sand<sup>10</sup>; ● Wilson, *et al.* (private communication)—Ottawa sand; ● Woodside & Cliffe—Ottawa sand<sup>10</sup>; - - - calculated—DeVries equation (11); — calculated—Kunii & Smith equation (12).

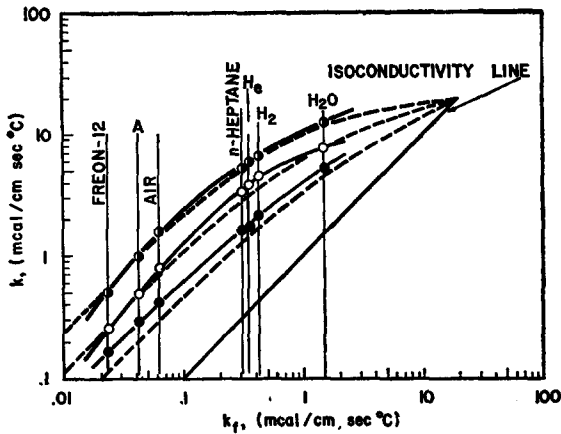


FIG. 6. Variation of effective thermal conductivity of unconsolidated quartz sands with the conductivity of the saturating fluid.  $\circ$  20/30 mesh Ottawa sand,  $\phi=0.361$ ;  $\bullet$  20/30 Ottawa & 140/200 Wassau,  $\phi=0.194$ ;  $\bullet$  140/200 Wassau sand,  $\phi=0.59$ ; --- calculated (DeVries' equation).

### EXPERIMENTAL RESULTS

Figure 5 shows some of the thermal conductivity data, obtained for the three quartz sand packs, plotted against porosity. The three groups of data correspond to air, oil (*n*-heptane), and water saturated conditions. In the case of the 59% porosity sand, the porosity decreased to 51.5% upon liquid saturation. The data of other investigators are also shown.

Figure 6 shows the effective thermal conductivities of the three sand packs plotted against the thermal conductivities of the saturating fluids on logarithmic scales. Also shown is the isoconductivity line, i.e., the line for which  $k_s = k_f$ . The conductivity of the solid particles of the pack  $k_s$  is determined by the intersection of the effective conductivity curve with the isoconductivity line. Unfortunately, the extrapolation of the curves from the water-saturated points to the isocon-

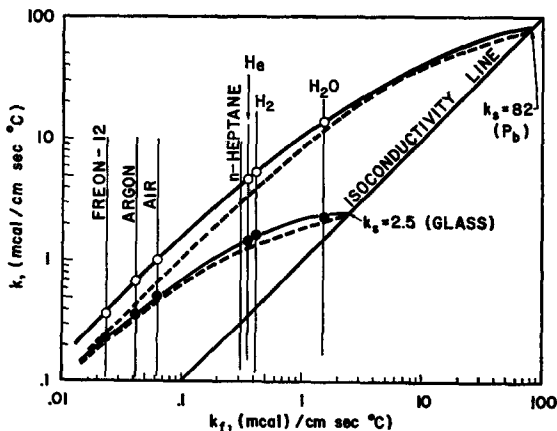


FIG. 7. Variation of effective thermal conductivity with the saturant conductivity for a lead shot and a glass bead pack.  $\circ$  Lead shot,  $\phi=0.379$ ,  $D_p=1.2$  mm;  $\bullet$  glass beads,  $\phi=0.380$ ,  $D_p=0.36$  mm; --- calculated (DeVries' equation).

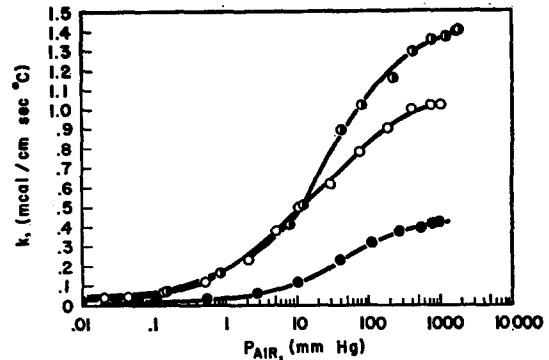


FIG. 8. Effective thermal conductivity of quartz sand packs as a function of the interstitial air pressure.  $\circ$  20/30 mesh Ottawa & 140/200 mesh Wassau sands,  $\phi=0.18$ ;  $\bullet$  20/30 Ottawa sand,  $\phi=0.33$ ;  $\bullet$  140/200 Wassau sand,  $\phi=0.59$ .

ductivity line is doubtful. One measurement was therefore made on the 20/30 Ottawa sand pack, saturated with mercury (under a capillary pressure of approximately 120 cm Hg to ensure that the pore space was more than 99% filled with mercury). The thermal conductivity of mercury is 20.0 mcal/cm sec $^{\circ}$ C at 30 $^{\circ}$ C.<sup>43</sup> The measured effective conductivity of the mercury-filled sand pack was 20.3 mcal/cm sec $^{\circ}$ C; however, too much reliance should not be placed on this result, since edge effects occurred relatively early in the measurement. The result does suggest that the assumption of 20 mcal/cm sec $^{\circ}$ C as the average solid conductivity of quartz grains is valid.

A similar plot of effective thermal conductivity versus saturant conductivity is shown in Fig. 7 for the lead shot and glass bead packs. All of the above measurements were conducted with the saturating fluid near atmospheric pressure.

The variation of the effective thermal conductivity with the pressure of the saturating air is shown in Fig. 8 for the three sand packs, and in Fig. 9 for the lead and glass bead packs, the air pressure being plotted on a logarithmic scale.

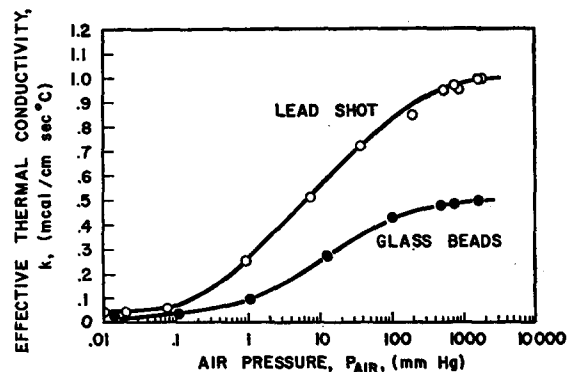


FIG. 9. Effective thermal conductivities of a lead shot and a glass bead pack as a function of the interstitial air pressure.

<sup>43</sup> W. H. McAdams, *Heat Transmission* (McGraw-Hill Book Company, Inc., New York, 1942), 2nd ed.



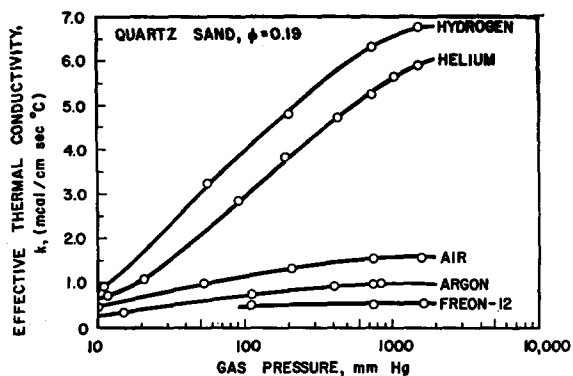


FIG. 10. Effective thermal conductivity of a low porosity quartz sand as a function of the interstitial gas pressure.

A similar plot is shown in Fig. 10 for one of the sand packs, over a more limited range of interstitial gas pressure, but with several different gases used as the saturating fluid.

## DISCUSSION

### Variation of $k$ with Gas Pressure

One of the points of interest concerning the data presented in Figs. 8 and 9 is the low value of the effective thermal conductivity *in vacuo*. The highest value of the resistor-model parameter  $b = k_{vac}/k_s$  is 0.0084 for the glass bead pack. The other four packs possess  $b$  values of 0.00155 or lower. Thus the neglect of the heat conduction through the grain contacts is warranted in the application of the resistor model equation and Kunii and Smith's equation to unconsolidated materials.

The kinetic theory expression for the thermal conductivity of a gas is<sup>44</sup>

$$k_f = A\rho c_v \bar{v} \lambda, \quad (22)$$

where  $A$  is a constant,  $\rho$  is the gas density,  $c_v$  is the specific heat at constant volume,  $\bar{v}$  is the mean molecular velocity, and  $\lambda$  is the mean free path. Normally, thermal conductivities of gases are independent of the gas pressure  $P$ , since  $\rho$  is directly proportional to  $P$ , and  $\lambda$  is inversely proportional to  $P$ . As the pressure is lowered, the mean free path approaches the size of the gas enclosure, and the linear dimension of the gas enclosure becomes an upper limit to the mean free path. Thus at low pressures, the gas conductivity becomes proportional to the pressure, since the inverse relation between  $\lambda$  and  $P$  no longer holds. In the case of a gas contained in a porous medium, such as the unconsolidated packs considered here, the linear dimension of the gas enclosure is some characteristic dimension of the pore space, which will be denoted by  $d$ . The effective mean free path  $\bar{\lambda}$  must depend upon  $d$  as well as the normal mean free path  $\lambda$ , since collisions between

gas molecules and the solid surface must be taken into account. It can be shown that  $\bar{\lambda}$  is given by the following expression:

$$\bar{\lambda} = \lambda d / (\lambda + d). \quad (23)$$

At high gas pressure, where  $\lambda \ll d$ ,  $\bar{\lambda} = \lambda$ ; at low gas pressures, where  $\lambda \gg d$ ,  $\bar{\lambda} = d$ . Thus, for air contained in a porous medium

$$\begin{aligned} k_f &= A\rho c_v \bar{v} \bar{\lambda} = A\rho c_v \bar{v} \lambda [d / (\lambda + d)] \\ &= k_{air} [d / (\lambda + d)], \end{aligned}$$

where  $k_{air}$  is the normal thermal conductivity of air (i.e., when  $\lambda \ll d$ ). Since  $\lambda = B/P$  ( $B = 0.00486$  for air when  $\lambda$  is expressed in cm and  $P$  in mm Hg),

$$k_f = k_{air} [Pd / (Pd + B)]. \quad (24)$$

Thus as the pressure is lowered,  $k_f$  decreases and hence the effective conductivity  $k$  of the pack must decrease as observed in Figs. 8–10.

To determine whether or not the rate of decrease of  $k$  with decrease in pressure is consistent with kinetic theory, Fig. 11 must first be examined. This figure shows some of the data of Figs. 6 and 7 plotted on a linear scale. It is apparent that, for low values of  $k_f$ , the data may be approximately represented by an equation of the form

$$k = Wk_f + k_{vac}, \quad (25)$$

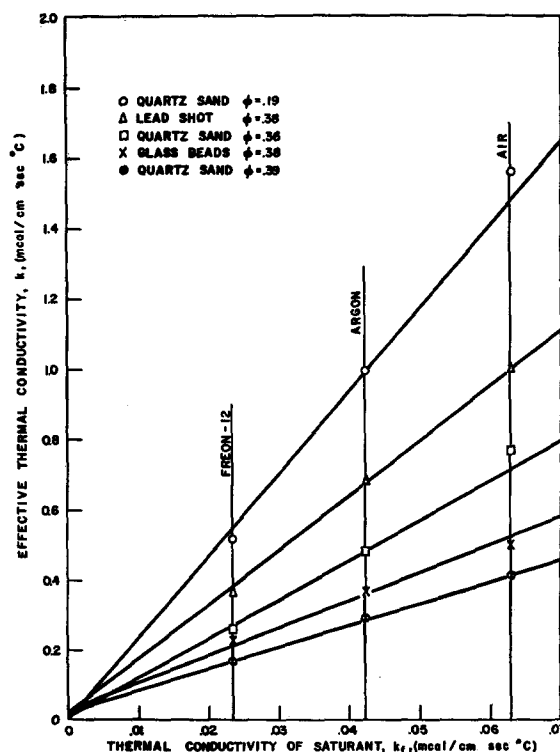


FIG. 11. Variation of effective thermal conductivity with the conductivity of saturating gas for low conductivity gases.

<sup>44</sup> E. H. Kennard, *Kinetic Theory of Gases* (McGraw-Hill Book Company, Inc., New York, 1938).

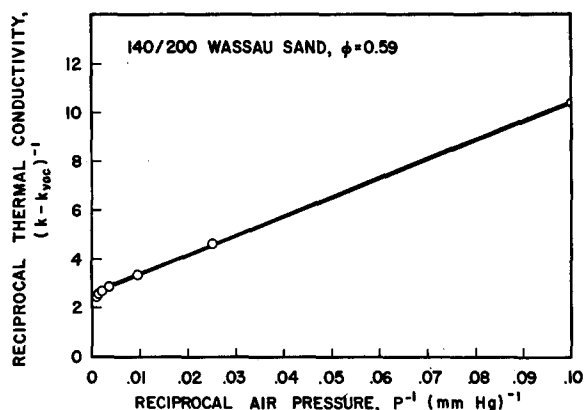


FIG. 12. Reciprocal thermal conductivity  $1/(k - k_{vac})$  plotted against reciprocal air pressure for a quartz sand pack.

where  $W$  represents the slope of the straight line drawn through each set of data.

Returning to Eq. (24), it follows that

$$k - k_{vac} = Wk_f = Wk_{air}[Pd/(Pd + B)]$$

or

$$1/(k - k_{vac}) = (1/Wk_{air})\{1 + [(1/P)(B/d)]\}. \quad (26)$$

Thus kinetic theory indicates that  $1/(k - k_{vac})$  should vary linearly with  $1/P$ . The experimental data do satisfy this relationship approximately as evidenced by Fig. 12, which is a plot of  $1/(k - k_{vac})$  against  $1/P$  for one of the sand packs. Furthermore a value for  $d$  may be obtained from such a plot. The values of  $d$  obtained are considerably smaller than the mean particle diameter  $D_p$ . The values of  $D_p/d$  are 68.1 (20/30 mesh sand), 61.4 (140/200 mesh sand), 72.6 for the glass bead pack, and 170 for the lead shot.  $d$  represents a characteristic dimension of the pore space from the point of view of molecular conduction in the gas. If it is assumed that the solid particles are spherical, it is easily shown that the above  $D_p/d$  values indicate that the part of the gas phase, which is of prime importance in heat conduction, extends from the contact point between adjacent grains out to a distance of roughly one-sixth of the grain radius. This critical region is even smaller in the case of lead shot, possibly because of the higher solid conductivity, or possibly because the lead-air system possesses a nonunit accommodation coefficient. In the case of the low-porosity two-component sand mixture, two straight lines fit the data quite well, on a  $1/(k - k_{vac})$  versus  $1/P$  plot. In this pack, the two most numerous types of particle contact are (a) small particle contacting small particle, and (b) large particle contacting small particle. Case (a) yields a value of 99 for  $D_p/d$ . For case (b), taking for  $D_p$  the harmonic mean of the two particle diameters, a value for  $D_p/d$  of 56 is obtained.

### VALIDITY OF THERMAL CONDUCTIVITY EQUATIONS

Figure 13 shows a plot of the dimensionless conductivity ratios  $y = k/k_f$  and  $x = k_s/k_f$  for the glass bead and lead shot packs. For comparison, the values calculated from the several thermal conductivity equations are also plotted ( $\phi = 0.38$ ). It is apparent that Maxwell's equation<sup>10</sup> predicts values for  $k$  which are too low, whereas both de Vries' equation<sup>11</sup> and Kunii and Smith's equation<sup>12</sup> agree fairly well with the data. Kunii and Smith's equation appears to underestimate  $k$  when  $k_s/k_f$  is small; de Vries' equation underestimates  $k$  when  $k_s/k_f$  is very large. The geometric mean equation overestimates  $k$  when  $k_s/k_f$  exceeds 20. The resistor model equation (13) (not plotted) assuming  $b=0$  and  $c=\phi^{1.3}$ , considerably underestimates  $k$ , predicting values slightly lower than those given by Maxwell's equation. Note how all the curves converge to the point  $x=1$ ,  $y=1$  with the same slope as required by Eq. (6). The plotting of both the lead shot and glass bead data on the same graph was possible since both packs possessed the same porosity.

The equations of de Vries, and Kunii and Smith are compared with the quartz sand data in Fig. 5. Again both equations are fairly consistent with the data. The rather abrupt change in slope of the Kunii and Smith curve at  $\phi=0.26$  is caused by the use of  $\epsilon_2$  for  $\epsilon$  for all values of  $\phi$  less than 0.26. Comparisons are also made in Figs. 6 and 7.

As mentioned above, the resistor model equation, using for  $c$  the reciprocal electrical formation factor, predicts effective conductivities considerably lower than those measured. It was decided, therefore, to calculate the values  $c$  must have in order to make the resistor model equation match the observed data (while retaining the approximation  $b=0$ ). The values of  $c$  thus calculated are remarkably constant for a given pack, varying only

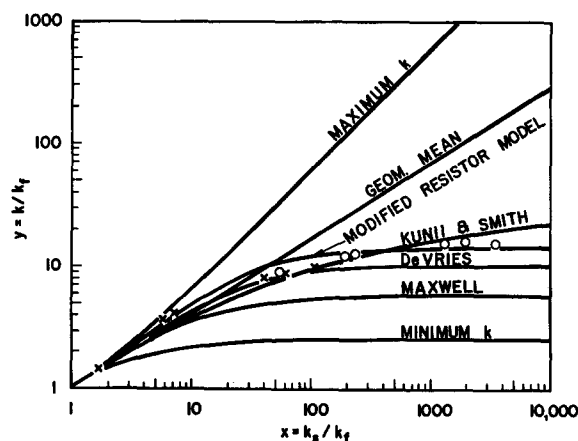


FIG. 13. Comparison of lead shot and glass bead conductivity data with the values calculated from the various conductivity equations.  $\circ$  lead shot,  $\phi=0.38$ ,  $K_s=82$  mcal/cm sec°C;  $\times$  glass beads,  $\phi=0.38$ ,  $K_s=2.5$  mcal/cm sec°C.

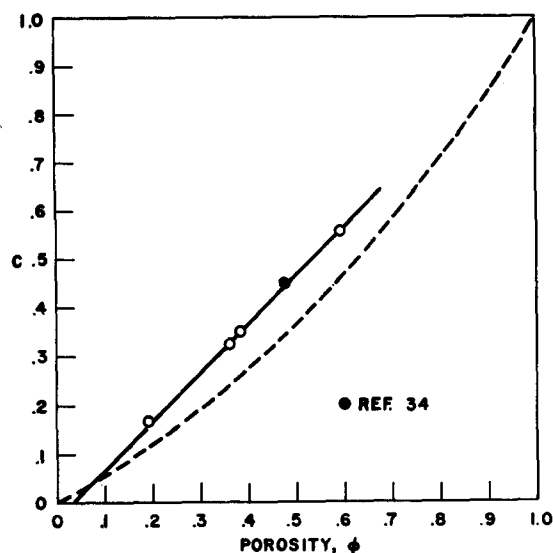


FIG. 14. Comparison of measured "thermal formation factor" with electrical formation factor for unconsolidated media. ---  $C = 1/F = \phi / (1.3219 - 0.3219\phi)^2$ , Slawinski electrical formation factor ( $K_f/K_s \rightarrow \infty$ ).

$$O \quad C = \frac{\phi K K_s + (1-\phi) K K_f - K_s K_f}{\phi K_s K_f + K K_s - 2 K_s K_f + (1-\phi) K_f^2}$$

reciprocal thermal formation factor  $K_f/K_s \sim 0.02$ .

slightly with  $k_s/k_f$  until the latter approaches unity. For example, for the 19.4% porosity sand pack, the seven calculated values of  $c$  varied between 0.1631 and 0.1683 while  $k_s/k_f$  varied from 855 to 13.3. A value for  $c$  was also calculated from the experimental data of Stephenson and Woodside<sup>45</sup> for a model of a cubic pack of spheres at a porosity of 47.6%. The values of  $c$  obtained from the experimental data are plotted against porosity in Fig. 14. The points may be represented quite well by the linear relation

$$c = \phi - 0.03. \quad (27)$$

To show the comparison between this measured "thermal formation factor" and the electrical factor, Slawinski's<sup>18</sup> equation is also plotted. The disagreement between the thermal and electrical  $c$  values is not altogether surprising, when one considers that the electrical factor is associated with systems of electrically non-conducting particles contained in an electrolyte (i.e.,  $k_s=0$ ,  $k_f \neq 0$ ), whereas in the thermal case the solid conductivity is never zero and in many practical cases much larger than  $k_f$ . In conclusion, the resistor model equation (13) if used with the auxiliary relations  $b=0$ ,  $c=\phi-0.03$ ,  $a=1-c$ , and  $d=(1-\phi)/a$ , predicts effective thermal conductivity values in fair agreement with those observed for unconsolidated media. This modified resistor model equation is plotted in Fig. 13.

<sup>45</sup> D. G. Stephenson and W. Woodside, Trans. Am. Soc. Mech. Engrs. 80, 1424 (1958).

## CONCLUSIONS

(1) The line heat source (probe) method is satisfactory for the determination of effective thermal conductivities of unconsolidated sands under a variety of test conditions. The measurements are rapid and reproducible to within one or two percent. All measurements were performed at room temperature with a single saturating fluid occupying the pore space.

(2) Effective thermal conductivities were measured for three unconsolidated quartz sand packs, ranging in porosity from 0.19 to 0.59. With water as the saturating fluid, the conductivities ranged from 12.3 to 5.17; with air as saturant (near atmospheric pressure) the conductivities ranged from 1.57 to 0.416 mcal/cm sec°C. The variation with porosity is greater the higher the conductivity of the saturating fluid (Fig. 5).

(3) Effective thermal conductivities were measured for two unconsolidated packs having the same porosity, but with solid particle conductivities differing by a factor of 33. The effect of the higher solid conductivity increased as the conductivity of the saturating fluid increased. The ratio of the two effective conductivities was 2.0 for air as the saturant, but was 6.05 for water as the saturant (Fig. 7).

(4) The effective thermal conductivity of an unconsolidated pack increases with the conductivity of the saturating fluid, the increase being in almost direct proportion when the saturant conductivity is small relative to that of the solid (Fig. 11).

(5) The effective conductivities *in vacuo* of all five packs studied were less than one-hundredth of the conductivities of the respective solid particles. As the saturating gas pressure was increased from the evacuated condition the effective conductivity increased, continuing to increase, in some cases, at pressures higher than atmospheric (Figs. 8-10). The variation with gas pressure was shown to be consistent with the kinetic theory of gases.

(6) From considerations based on kinetic theory, it was determined that the characteristic dimension of the pore space, with respect to heat conduction in the gas occupying this space, is smaller than the mean particle diameter by a factor of roughly 100. It was concluded that the part of the gas phase, which is of prime importance in heat conduction, extends from the contact points between the solid particles out to a distance of roughly one-sixth of the particle radius.

(7) Equations which relate the effective conductivity of a two-phase medium to the conductivities and concentrations of the constituent phases were reviewed in the light of the observed data (Fig. 13). The geometric mean equation overestimates the effective conductivity when  $k_s/k_f$  exceeds about 20.

(8) Maxwell's equation underestimates the effective conductivity. However, de Vries' equation (based on an extension of Maxwell's equation by Burger and Eucken) and the equation of Kunii and Smith both

show fair agreement with the observed values over the ranges of porosity, saturant conductivity and solid particle conductivity studied.

(9) The resistor model equation of Wyllie and Southwick, used in conjunction with a value of the parameter

$c$  determined electrically, leads to effective thermal conductivity values considerably lower than those measured. Good agreement with the observed data is achieved if  $c$  is calculated from the relationship  $c = \phi - 0.03$  obtained empirically.

## Thermal Conductivity of Porous Media. II. Consolidated Rocks

W. WOODSIDE AND J. H. MESSMER

*Gulf Research and Development Company, Pittsburgh, Pennsylvania*

(Received March 13, 1961)

Measurements have been made of the effective thermal conductivity of porous sandstones. The method is based on the transient heating effect resulting from use of a line heat source. Data are presented for six sandstones ranging in porosity from 3 to 59% and show the variation of thermal conductivity with porosity, the conductivity of the saturating fluid, the pressure of the gas filling the pore space, and overburden pressure. The results are compared with those previously obtained for unconsolidated sands. All samples, except one, exhibited a lower thermal conductivity when saturated with a gas at atmospheric pressure than when saturated with a liquid of the same conductivity as the gas. An explanation for this effect, in terms of the kinetic theory of gases, is advanced and substantiated by other data. Finally, the validity of certain equations for the thermal conductivity of two-phase systems is examined; the weighted geometric mean of the two constituent conductivities is found to agree well with the measured effective conductivities.

### INTRODUCTION

PART I of "Thermal conductivity of porous media" described the theoretical background, the method used for thermal conductivity measurement, and the results obtained for several unconsolidated media. Part II presents the results obtained for consolidated rock samples.

### EXPERIMENTAL PROCEDURE

The rock samples were cylinders  $6\frac{1}{2}$  in. long and at least 3 in. in diameter. A hole 6 in. long and  $\frac{3}{32}$  or  $\frac{1}{8}$  in. in diameter along the central axis of the cylinder is necessary to accept the probe. All samples, except one, were successfully drilled. The exception, Berkeley sandstone, was very hard. This sample was finally cut in two longitudinally, and grooves of the appropriate dimensions were ground in the matching faces of the halves, which were then reassembled and held together by steel strips.

Wood's metal (mp=61°C) inserted between probe and specimen was found to eliminate contact resistance of probe to rock. The metal expands upon solidification, effecting a good bond between probe and rock. No evidence of metal penetration into the rock pores was found. The probe is easily removed, when necessary, by heating. All data presented here were obtained in this way. The probe length-to-diameter ratio is 64 or 48 for holes of diameter  $\frac{3}{32}$  or  $\frac{1}{8}$  in., respectively; however, this is still larger than the 30 theoretically required.<sup>1</sup>

For thermal conductivity measurements under a simulated overburden pressure, the sample, with probe

in place, was encased in a half-inch thickness of an impervious rubber (Dow Corning Silastic RTV 501), placed in a pressure vessel, and subjected to hydraulic pressure. The apparatus is shown in Fig. 1. The electrical leads to the probe and high-pressure tubing, connected to the inside of the sample, were brought out through the rubber and pressure vessel, permitting the internal gas pressure to be varied. The tubing-pore space

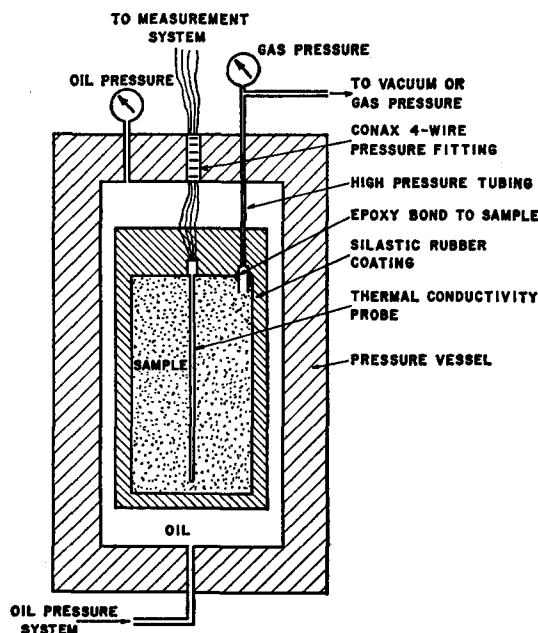


FIG. 1. Schematic diagram of apparatus for measurement of thermal conductivity as a function of overburden pressure.

<sup>1</sup> J. H. Blackwell, Can. J. Phys. 34, 412 (1956).